Contents lists available at SciVerse ScienceDirect

European Polymer Journal

journal homepage: www.elsevier.com/locate/europolj

Crystallization of isotactic polypropylene containing beta-phase nucleating agent at rapid cooling

CrossMark

Ayret Mollova [a], René Androsch [a,*], Daniela Mileva [b], Markus Gahleitner [b], Sergio S. Funari [c]

[a] Martin-Luther-University Halle-Wittenberg, Center of Engineering Sciences, D-06099 Halle/Saale, Germany
[b] Borealis Polyolefine GmbH, Innovation Headquarters, A-4021 Linz, Austria
[c] Hasylab at DESY, Notkestr. 85, D-22607 Hamburg, Germany

ARTICLE INFO

ABSTRACT

The crystallization behavior of isotactic polypropylene containing a β-phase nucleating agent has been investigated, focusing on evaluation of the effects of cooling rate and/or supercooling of the melt on the generation of different polymorphs. It has been found that β-crystals only form on cooling the melt at rates lower than about 50 K s^{-1} while cooling at rates between 50 and 300 K s^{-1} leads to formation of α-crystals; even faster cooling is connected with mesophase formation or vitrification of the entire melt. Fast scanning chip calorimetry revealed different mechanisms of nucleation at low and high supercooling. In comparison to non-nucleated iPP the presence of the β-phase nucleating agent only affects the crystallization kinetics at low supercooling, supporting the idea that ordering at high supercooling is governed by homogeneous nucleation. β-crystals, formed initially on slow cooling, melt below about 420 K on slow heating, followed by formation of few α-crystals on continuation of heating. The mesophase initially formed on fast cooling and aging at ambient temperature, in contrast, re-crystallizes directly into α-structure. The results of the present work provide comprehensive information about the condition of formation and the stability of different polymorphs in isotactic polypropylene containing a β-phase nucleating agent.

© 2013 Elsevier Ltd. All rights reserved.

1. Introduction

The crystalline phase in semicrystalline isotactic polypropylene (iPP) may adopt different structures and morphologies depending on the condition of crystallization [1–3]. Slow cooling of the melt at rates lower than about 10^2 K s^{-1}, or isothermal crystallization at temperatures higher than about 330 K typically leads to formation of the thermodynamically stable monoclinic α-form [4,5]. The formation of α-crystals from the supercooled quiescent melt proceeds via spherulitic growth of lamellae. Due to lamellar branching, radially and tangentially oriented lamellae are observed, with their ratio depending on the crystallization temperature [4–9]. Cooling the melt at rates faster than 10^2 K s^{-1} to temperatures between the glass transition temperature of 270 K and 330 K, results in formation of a mesophase [4,5] which has been described as a conformationally disordered glass [10,11]. The mesophase is of non-lamellar morphology [12–14], and converts on heating to α-crystals with the initial non-spherulitic superstructure and particle-like habit of the mesophase preserved [15–20].

The β-structure of pseudo-hexagonal symmetry may be observed at special conditions of crystallization including crystallization in a temperature gradient, or crystallization of oriented melt [1,7,21–25]. The growth rate of β-crystals is higher than that of α-crystals in a wide temperature range between 378 and 414 K [8], which has been attributed to a lower surface free energy penalty on addition of molecular stems at the 110 growth face of the β-crystals,

* Corresponding author. Tel.: +49 3461 46 3762; fax: +49 3461 46 3891.

E-mail address: rene.androsch@iw.uni-halle.de (R. Androsch).

that is, to presence of favorable secondary nucleation sites [26,27]. However, since the rate of primary nucleation of the β-phase is lower than that of α-crystals, semicrystalline iPP containing β-crystals typically cannot be obtained without addition of special heterogeneous β-phase nucleators [28–30]. The β-phase exhibits a trigonal unit cell [31], and forms negatively birefringent radial or banded spherulites on crystallization from the quiescent melt [7]; the structure development and lamellar arrangement has been demonstrated in detail elsewhere [21]. The β-phase exhibits a unique melting behavior such if cooled below a critical temperature of about 375 K it re-crystallizes into the α-form during heating. The re-crystallization to α-crystals does not occur in samples which were not cooled below this critical temperature and the β-crystals melt separately; this phenomenon has been named "melting memory effect" [32].

From application point-of-view, iPP containing β-crystals exhibits a lower modulus of elasticity, a lower yield stress, and a higher ductility than iPP containing α-crystals; furthermore, the impact strength and toughness are higher [33–38]. It has been shown that a variation of the processing conditions affects both the formation of the β-modification and the related mechanical performance of iPP [39], however without a detailed investigation of the involved thermal history.

Finally, the γ-structure develops in low molar mass fractions of polydisperse iPP, in random copolymers with shortened isotactic sequences, or in presence of high pressure. The γ-phase is of orthorhombic symmetry, and typically forms in conjunction with the α-phase, being mixed within spherulites. Since α- and γ-crystallization leads to simultaneous occurrence of radially and tangentially aligned lamellae within spherulites, the net birefringence of spherulites is lower than that of β-spherulites, permitting straightforward identification of the latter by polarizing optical microscopy [2,3,40–42].

With the present work we attempt to shed further light onto the crystallization behavior of iPP containing a β-nucleator. As far as we are aware, systematic studies of the effect of cooling rate and supercooling of the melt on the crystallization process including generation of different polymorphs and the kinetics of crystallization have not been performed yet. For non-nucleated iPP it is known that α-crystals form via heterogeneous nucleation at temperatures higher than about 330 K while at lower temperatures a mesophase develops via homogeneous nucleation, or via heterogeneous nucleation but at different sites than are active at higher temperatures. The research object of identification of different nucleation mechanisms in crystallizable materials and in particular polymers has been discussed in detail at the 12th Lähnwitzseminar entitled "Interplay between Nucleation, Crystallization, and the Glass Transition", however, without having achieved a unanimous opinion whether homogeneous nucleation in crystallizable polymer is detectable, or not [43]. The minimum half-times of crystallization and mesophase formation of about 0.2 and 0.05 s [44,45] are observed at temperatures of about 340 and 300 K, respectively, leading to a bimodal dependence of the crystallization rate versus temperature [44–47]. It is emphasized that mesophase

formation at temperatures close to the glass transition temperature is faster than crystallization due to increased primary nucleation rate but not due to increased growth rate. With the assumption that mesophase formation of iPP at temperatures lower than 330 K occurs via homogenous nucleation, the addition of a heterogeneous nucleator is expected to affect only the slower crystallization kinetics at higher temperature.

Analysis of the crystallization behavior of nucleated iPP in a wide range of different crystallization conditions including different supercooling and rates of cooling is assumed to provide valuable information about generation of different polymorphs. The efficiency of heterogeneous nucleators, which in the context of the present study is considered as the capability of a nucleating agent to promote crystallization of a specific crystal form, depends on the temperature dependencies of both the crystal form intended to generate by the addition of the nucleating agent, and the crystal form to be replaced. In the particular case of intended formation of β-crystals in iPP, solidification of the supercooled melt must occur at temperatures at which α-crystal nucleation and crystal growth is slower than in case of the β-form. It will be shown that β-crystals, α-crystals and mesophase may form as a function of the conditions of solidification in β-nucleated iPP, which implies that the efficiency of the used nucleating agent to produce measurable amount of β-phase is limited to certain conditions.

Finally, in this work we investigated the stability and the reorganization behavior of the different polymorphs of β-nucleator containing iPP, with the different polymorphs developed by variation of the condition of melt solidification. It is expected, based on earlier reports, that β-crystals reorganize to α-structure [22,32,48] and that α-crystals evident at ambient temperature increase their stability without changing the crystal structure on slow heating. The reorganization behavior of the mesophase of iPP containing a β-nucleator, in contrast, has not been studied yet. In non-nucleated iPP, the mesophase transforms to α-crystals on slow heating, starting at about 350 K [11,15–17]. It has been suggested that the mesophase–α-crystal transition proceeds by removal of conformational defects/helix reversals at local scale within existing domains, and without prior complete disordering/isotropization of the mesophase [20]. The enthalpy of the mesophase–α-crystal transition is rather low [49,50], which implies that the mesophase seemingly can be considered as a precursor for α-crystal formation. We assume that the presence of β-nucleator in semimesomorphic iPP, that is, in iPP containing mesophase besides amorphous phase, does not affect the mesophase–α-crystal transition on slow heating, which however, we intended to prove within the present work. Fast heating, in contrast, would lead to complete disordering of the mesophase at around 350 K [51], and then β-crystals may form on annealing the supercooled melt.

Summarizing the scope of this work, we intend to provide new information about the nucleation efficiency of γ-quinacridone as a widely used nucleator to obtain β-crystals in iPP [28–30,52,53]. In an extension of earlier work, we focus on analysis of the crystallization behavior

of β-nucleated iPP at rapid cooling conditions, and at high supercooling, that is, at conditions, which cannot be emulated using standard differential scanning calorimetry (DSC), and which are valid on melt processing. As such we employed, among others, the novel technique of fast scanning chip calorimetry (FSC), with the particular instrument used allowing cooling at rates up to 2000 K s^{-1}, and monitoring/quantification of isothermal crystallization/ordering processes even at temperatures of fastest growth rate, that is, of transitions which are completed within few hundreds of a second. In addition, wide-angle X-ray scattering was used to gain information about the specific polymorphs forming as a result of a specific cooling history, using samples which were prepared in a special quenching device. The reorganization behavior of the various polymorphs generated by variation of the cooling history, finally, was analyzed by temperature-resolved wide-angle X-ray scattering.

2. Experimental section

2.1. Material and preparation

In the present work we employed a commercial β-nucleated iPP grade BE60 of Borealis AG (Austria) which has been studied before in comparison to a non-nucleated grade [54]. The material is based on a Ziegler–Natta type iPP with a weight average molar mass of 1070 kDa and a polydispersity of 6.5, containing γ-quinacridone as β-phase nucleating agent at a concentration of less than 100 ppm; the effect of the catalyst system on the crystallization behavior of iPP is reported in detail elsewhere [55]. The material was received in form of pellets, and was in a first step compression-molded to films with a thickness of 100 μm using a Perkin Elmer hydraulic press in combination with a Lot-Oriel/Specac film maker die and heating accessory. Further preparation steps to fit the requirements of the analytical tools used in this work are described below on description of the instrumentation.

2.2. Instrumentation

2.2.1. Quenching device
Films of different cooling history were prepared using a home-made device for fast film cooling. A chromel–alumel μ-thermocouple from Omega with a wire diameter of 50 μm was placed between two of the initially compression-molded films and connected to a data acquisition system to obtain the sample temperature at a sampling rate of 20 Hz during the cooling step. The 200 μm thick films with the embedded thermocouple were positioned between two copper plates with a thickness and area of 300 μm and 30 × 35 mm^2, respectively, and fixed by two spring clips. The sandwich was inserted into a custom-made tube oven (Horst GmbH, Germany) which was pre-heated to a temperature of 493 K, and then rapidly transferred into different cooling media. In this work we used ice water, liquid nitrogen, cold air in a partially filled liquid nitrogen Dewar vessel, and air. The use of ice water allowed cooling at 180 and 155 K s^{-1} with the different values obtained due

slightly different film thickness. The use of liquid nitrogen, cold air above liquid nitrogen, and air led to cooling rates of 54, 3 and 0.4 K s^{-1}, respectively. By decreasing the thickness of the polymer film from 200 to 100 μm, and replacing the copper plates by thin aluminum foils, a cooling rate of 1400 K s^{-1} was achieved on quenching in ice water. Note that the sample temperature decreases non-linearly to the target temperature of the specific cooling medium as a function of time which implies that the cooling rate is a function of temperature. The above reported cooling rates are valid at a temperature of 343 K, based on a suggestion in the literature considering that the temperature of maximum crystallization rate of iPP is around 343 K [56]. The films of different cooling history were subsequently analyzed by wide-angle X-ray scattering (WAXS), to get information about the crystal structure, and their stability/reorganization behavior upon heating.

2.2.2. Wide-angle X-ray scattering (WAXS)
We employed a Seifert-FPM URD 63 diffractometer, operated in transmission mode. The wavelength of the X-rays was 0.15418 nm, and the scattered intensity was recorded using a scintillation counter. Further, temperature-resolved X-ray experiments were performed at the A2 SAXS/WAXS beamline at Hasylab/DESY (Germany), using monochromatic X-rays with a wavelength of 0.15 nm and a sample-detector distance of 140 mm; for detection of scattering data we employed two-dimensional MarCCD165 detector. Several layers of the polymer film of defined cooling history were wrapped into aluminum foil, and inserted into a temperature-controlled sample holder such that the normal of the sample was oriented parallel to the beam with a size of about 2 mm (vertical direction) × 3 mm (horizontal direction). Samples of different cooling history, initially at room temperature containing β-crystals, α-crystals, or mesophase were heated in vacuum atmosphere to 453 K at a rate of 5 K min^{-1} while acquiring X-ray frames each 30 s.

2.2.3. Differential scanning calorimetry (DSC)
DSC experiments were performed to measure temperatures of crystallization on slow cooling the relaxed melt at rates between 1 and 20 K min^{-1}. Heat-flow rate data were collected using a heat-flux DSC 820 from Mettler-Toledo, equipped with the liquid nitrogen accessory for controlled cooling. The sample mass was about 2.5 mg, and for encapsulation we used the small 20 μL aluminum pans from Mettler Toledo. The furnace of the DSC was purged with nitrogen gas at a flow rate of 80 mL min^{-1}, as recommended by the instrument provider. The instrument was calibrated as described in text books [57], using indium and zinc as calibration standards.

2.2.4. Fast scanning chip calorimetry (FSC)
FSC experiments were performed to get information about the kinetics of crystallization of iPP containing β-phase nucleating agent. The crystallization temperature was measured in non-isothermal experiments at cooling rates between 2×10^0 and 2×10^3 K s^{-1}. Prior to cooling, a relaxed melt was obtained by heating to 493 K and isothermal holding for a period of 0.1 s. The effect of the

equilibration time of the melt had been checked by analysis of the crystallization temperature on cooling at $10 \, K \, s^{-1}$, after relaxation the melt for 0.1, 0.5, 60 and 180 s. Variation of the melt-residence time did not affect the crystallization temperature. Isothermal crystallization experiments were performed in a wide temperature range between 283 and 373 K, to obtain characteristic times of crystallization/ordering. The sample was cooled at high rate of $2 \times 10^3 \, K \, s^{-1}$ to the temperature of analysis, to ensure presence of non-ordered supercooled melt at the beginning of the isothermal segment. Note that the various isothermal crystallization/ordering experiments at different temperature were performed in a single measurement. After isothermal crystallization/ordering at 283 K, the sample was cooled to 233 K and re-heated to 493 K at a rate of $10^3 \, K \, s^{-1}$, before renewing of equilibration the melt and approaching the next crystallization/ordering segment at 10 K higher temperature. Variation of the sequence of different crystallization temperatures did not affect the results.

We used a Flash DSC 1 from Mettler-Toledo in conjunction with a Huber intercooler TC45. The preparation of specimens included cutting of thin sections with a thickness of 10–15 µm from the as-received pellet, followed by decreasing the lateral size of the thin section to about 100 µm. Before the specimen was loaded into the calorimeter, a thin layer of silicon oil was spread on the membrane of the sample calorimeter, in order to improve the thermal contact to the sample. Furthermore, the sensor was subjected to a conditioning procedure by multiple heating and cooling cycles, and a temperature-correction of the factory pre-calibrated sensor considering the specific thermal environment like gas flow or heat-sink temperature, using a temperature–time program predefined by the instrument provider. The furnace was purged with dry nitrogen gas at a flow rate of $30 \, mL \, min^{-1}$ to warrant reproducible heat-loss conditions, and to avoid thermal-oxidative degradation of the sample and icing on cold instrument parts. Estimation of the sample mass has been done by comparison of measured, absolute heat capacities with specific values available in the ATHAS data base [58], using data measured at temperatures higher than the melting temperature. Further instrument information is reported in the literature [59,60].

3. Results and discussion

3.1. Effect of cooling history on X-ray structure of iPP containing β-phase nucleating agent

For evaluating the effect of cooling rate on the WAXS structure of samples of iPP containing β-nucleating agent, the isotropic melt was quenched in different media/cooling agents, as described in Section 2. Fig. 1 shows WAXS data obtained on the various samples of different cooling history, with the effective cooling rate at 343 K indicated at the right-hand side of each curve. Slow cooling at 0.4, 3, and $58 \, K \, s^{-1}$ led to formation of β-crystals, as is recognized with the strong peaks at 16.0 and 21.1 deg 2θ. These samples do not contain α-crystals since their characteristic
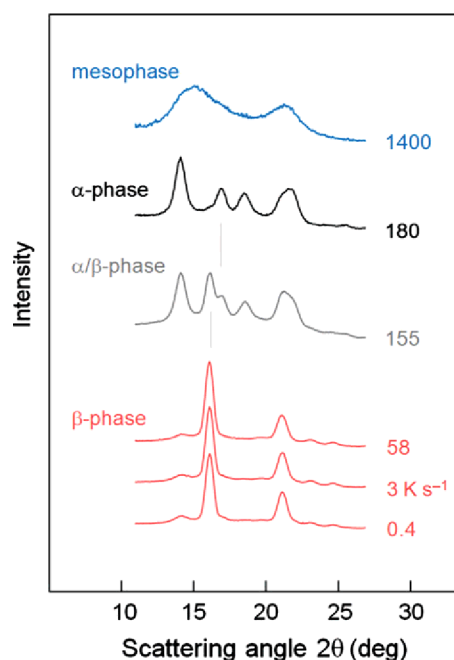

Fig. 1. WAXS diagrams obtained on samples of iPP containing β-phase nucleating agent. The isotropic melt was cooled at different rates as is indicated at the right-hand side of each curve.

peaks are not detected. If the cooling rate is increased to $155 \, K \, s^{-1}$ then both α- and β-crystals were formed on cooling the melt. The presence of β-crystals in this preparation is indicated with the scattering peak at 16.0 deg 2θ, while co-existence of α-crystals is evidenced with the peaks at 14.1, 16.9, 18.6, and 21.2/21.8 deg 2θ. Approximately 1/3 of the total crystal fraction in this sample is β-phase, as it was calculated based on a suggestion by Turner Jones et al. [2]. Further increase of the cooling rate to $180 \, K \, s^{-1}$ almost completely suppresses the formation of β-crystals, that is, the sample mainly contains α-crystals. Obviously, the β-phase nucleating agent is not effective when cooling the melt at rates faster than about $200 \, K \, s^{-1}$, and the material crystallizes as without the special β-phase nucleating agent. From prior work about the crystallization behavior of non-nucleated iPP it is known that α-crystals cannot form when cooling faster than a few hundred $K \, s^{-1}$ [4,5,11,56]. Instead, a mesophase forms at high supercooling which is confirmed with the quenching experiment using a rate of cooling of $1400 \, K \, s^{-1}$. Note that quenching the melt at this rate to a temperature below the glass transition temperature of about 260–270 K leads to its complete vitrification. Subsequent heating of the glass to ambient temperature, that is, to a temperature above the glass transition, however, immediately leads to ordering and formation of the mesophase.

Summarizing the WAXS analysis of samples of iPP containing γ-quinacridone as β-phase nucleating agent cooled at largely different rates between 0.4 and $1400 \, K \, s^{-1}$, we conclude that the nucleating agent is only efficient though not necessarily inactive on cooling at rates lower than about $100 \, K \, s^{-1}$. Note again that on fast cooling the nucleating agent may still be active; however, due to the low

growth rate of the β-phase with respect to that of the α-phase, in combination with the rather short residence time of the system in the temperature range between about 370 and 410 K, the β-phase may just become invisible due to its low fraction. If the cooling rate exceeds about 100 K s^{-1} then β-crystal formation is replaced by formation of α-crystals. We assume, however, that α-crystals on cooling form only in a narrow cooling-rate range of few hundred K s^{-1} since even faster cooling leads to suppression of crystallization.

3.2. Non-isothermal fast scanning chip calorimetry

Fig. 2 shows FSC heat-flow rate data as a function of temperature recorded on cooling iPP containing β-phase nucleating agent at different rate, with the cooling rate indicated at the right-hand side of each curve. We investigated a total of four different samples of largely different sample mass between 90 and 685 ng; the curves shown in Fig. 2 were obtained on a sample with a mass of 90 ng and can be considered as representative. A single crystallization event is detected on cooling at rates between 2 and 100 K s^{-1}. The crystallization temperature is about 390 K on cooling at 2 K s^{-1} and decreases to about 360 K on cooling at 100 K s^{-1}. Based on the knowledge gained from the X-ray data shown in Fig. 1, we assume that cooling at rates between 2 and 100 K s^{-1} resulted in formation of β-crystals.

Further increase of the cooling rate is connected with a change of the peak form in the FSC cooling curves. In particular on cooling at 200 and 400 K s^{-1} the crystallization process seems to consist of two different events since the exothermic peak is not only broadened toward lower temperature but also shows a distinct shoulder at the high-temperature side. With the red and gray dotted curves is indicated that the overall peak may be de-convoluted to reveal formation of β- and α-crystals, respectively. The interpretation of FSC curves recorded on cooling at rates of few hundred K s^{-1} is based on the observation of co-formation of α- and β-crystals after ballistic cooling at a rate of 155 K s^{-1} at 343 K (see Fig. 1). The minor mismatch of observation of co-formation of α- and β-crystals at a rate of 155 K s^{-1} at 343 K in the quenching experiment of Fig. 1, and at rates equal or faster 200 K s^{-1} in the FSC experiment of Fig. 2, likely, is related to ballistic and linear cooling, respectively; in the quenching experiment to obtain films for X-ray analysis, the cooling rate at the crystallization temperature of 360 K is around 200 K s^{-1} as in FSC analysis.

Further increase of the cooling rate to 600 and 1000 K s^{-1} leads to a distinct decrease of the observed enthalpy of transition, and further extension/broadening of the crystallization/ordering process to lower temperature. Samples cooled at rates faster than 600 K s^{-1} to below the glass transition temperature, eventually are nearly fully amorphous. This result, however, is not in contrast with the observation of rather large amount of mesophase after quenching at 1400 K s^{-1} and annealing at ambient temperature; annealing at ambient temperature leads to conversion of amorphous structure to mesophase.
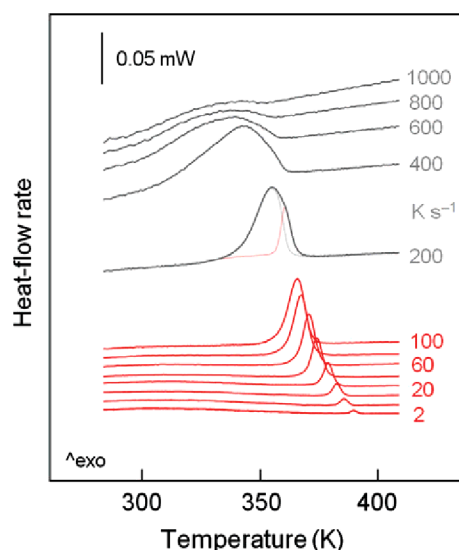

Fig. 2. FSC curves, heat-flow rate as a function of temperature, obtained on cooling a sample of iPP containing β-phase nucleating agent at different rates. The cooling rate is indicated at the right-hand side of each curve. Red color is used to indicate the range of cooling rates leading to formation of β-crystals. (For interpretation of the references to colour in this figure legend, the reader is referred to the web version of this article.)
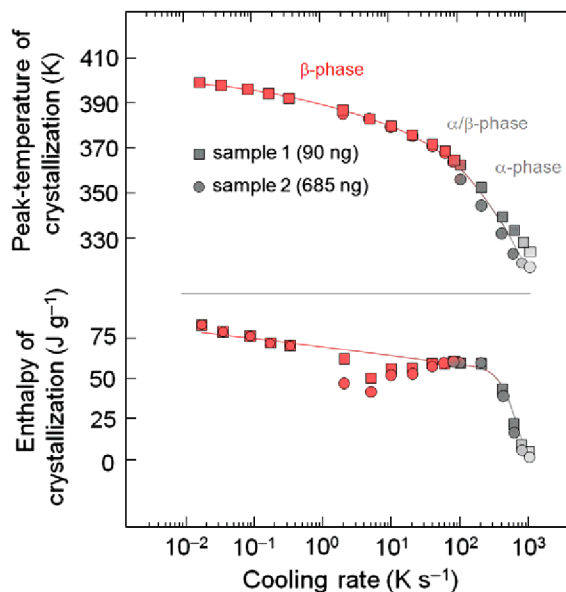

Fig. 3. Peak-temperature (top) and enthalpy of crystallization (bottom) of iPP containing β-phase nucleating agent as a function of the cooling rate. Red color is used to indicate the range of cooling rates leading to formation of β-crystals while gray colored data points indicate formation of α-crystals. (For interpretation of the references to colour in this figure legend, the reader is referred to the web version of this article.)

The cooling curves of Fig. 2 were analyzed quantitatively with regard to the peak-temperature and enthalpy of crystallization/ordering. Fig. 3 shows in the top part the peak-temperature and in the bottom part the enthalpy of crystallization/ordering, both as a function of cooling rate. In addition to data obtained by FSC on cooling at rates

between 2 and 1000 K s^{-1}, DSC data collected on cooling between 0.0167 and 0.3 K s^{-1} are also included. Color-coding of data points is in accord with the X-rays scans of Fig. 1; red colored data points refer to formation of β-phase and gray colored data points indicate formation of α-crystals. The plots contain data obtained on two samples of largely different mass, providing confidence that errors due to changed heat transfer conditions are negligible. In addition, we placed a piece of Indium on top of the polymer, to confirm that the observed decrease of the phase transition temperature with increasing cooling rate is not due to thermal lag effects. The crystallization temperature of the Indium remained constant within 2 K on increasing the cooling rate from 2 to 1000 K s^{-1}. Both the peak temperature and enthalpy of crystallization decrease with increasing cooling rate. Similar decreases have been observed for unmodified iPP; however, in case of the present investigation of iPP containing β-phase nucleating agent, non-isothermal mesophase formation was not detected, as is explained below. The data of Fig. 3 confirm the conclusion drawn from the X-ray experiments of Fig. 1 of lost efficiency of the β-phase nucleating agent to produce a large fraction of β-phase if the cooling rate exceeds about 100 K s^{-1}, ultimately caused by decrease of the crystallization temperature below 370 K. The enthalpy of crystallization decreases from a plateau value of about 60–70 J g^{-1} on cooling slower than 100 K s^{-1} to almost zero in a narrow cooling-rate range from 100 to 1000 K s^{-1}, being accompanied by replacement of formation of β-crystals to formation of α-crystals.

3.3. Isothermal fast scanning chip calorimetry

Fig. 4 shows FSC heat-flow rate data recorded as a function of time during isothermal crystallization/ordering. The sam-
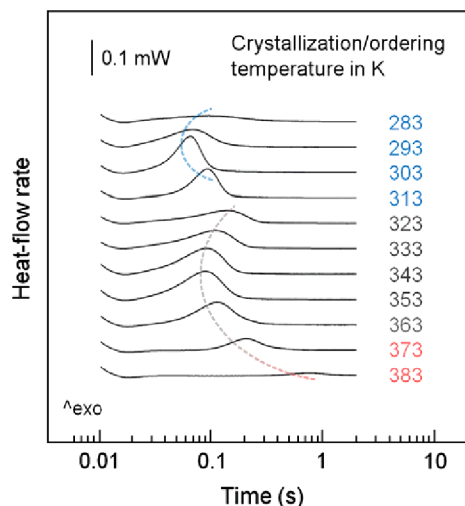
ple has been cooled from the melt at a rate of 2000 K s^{-1} to the various crystallization/ordering temperatures. Isothermal holding of the temperature at 383 K leads to crystallization after about 0.4 s with the maximum of the crystallization rate, as is given with the maximum of the curve, observed after about 0.8 s. Reducing the temperature leads to faster crystallization as is indicated with the appearance of the peak at shorter time; at temperatures of crystallization of 343 and 353 K, the peak-time of crystallization is about 0.1 s. Further decrease of the crystallization temperature first leads to a slowing down of the phase transition, before at temperatures lower than 313 K a reacceleration is observed. The bimodal distribution of the peak-time of crystallization/ordering has in the past been related to a change of the nucleation mechanism, from heterogeneous nucleation at high temperature to homogeneous nucleation at low temperature. We assume, based on the information gained by Figs. 1–3 that isothermal crystallization at temperatures higher than 360–370 K led to formation of β-crystals while crystallization between 320 and 360 K is connected with formation of α-crystals. The low-temperature process proceeding via homogeneous nucleation is known to yield mesophase.

Fig. 5 is a plot of the peak-time of crystallization/ordering of unmodified (light gray filled symbols) and iPP containing β-phase nucleating agent (red, dark gray and blue filled symbols) as a function of temperature. In both cases, for unmodified iPP and iPP containing β-phase nucleating agent, a bimodal distribution of the peak-times of crystallization/ordering is observed with the two distinct minima at about 340–350 and 300 K. The minimum at 340–350 K is related to formation of crystals via heterogeneous nucleation while the minimum at 300 K is related to mesophase formation via homogeneous nucleation. In the temperature range of homogeneous nucleation between the glass transition temperature and around 320 K, data collected on unmodified iPP and iPP containing β-phase nucleating agent are indifferent, and a minimum peak-time of ordering of about 0.05 s is observed. In other words, the β-phase nucleating agent does not affect the rate of mesophase
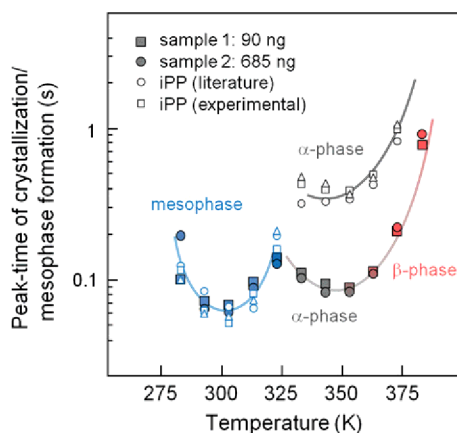

Fig. 4. Heat-flow rate as a function of time recorded during isothermal crystallization/ordering of iPP containing β-phase nucleating agent. The crystallization/ordering temperature is indicated at the right-hand side of each curve. Color-coding is in accord with Fig. 1, that is, red and gray colors indicate formation of β- and α-crystals, respectively, while blue color indicates formation of mesophase. (For interpretation of the references to colour in this figure legend, the reader is referred to the web version of this article.)

Fig. 5. Peak-time of isothermal crystallization/ordering of iPP containing β-phase nucleating agent as a function of temperature. For comparison, the plot contains with the light gray symbols data obtained on an unmodified iPP [44].
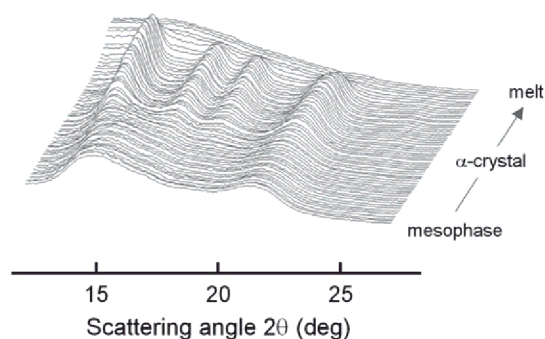
Fig. 6. Series of WAXS diagrams recorded on heating initially semimesomorphic iPP containing β-phase nucleating agent. The heating rate is 5 K min⁻¹. The front and back curves were recorded at 293 and 443 K, respectively.

Fig. 7. Series of WAXS diagrams recorded on heating initially semicrystalline iPP containing β-crystals. The heating rate is 5 K min⁻¹. The front and back curves were recorded at 293 and 453 K, respectively.

formation at high supercooling. In contrast, the rate of crystallization at temperatures higher than about 330 K is remarkably lower in unmodified iPP. We observed a minimum peak-time of crystallization of about 0.2 s in neat iPP while the peak-time is reduced to about 0.08 s in iPP containing β-phase nucleating agent.

The observation of almost identical peak-times of crystallization and ordering of 0.08 and 0.05 s, respectively, in iPP containing β-phase nucleating agent we consider as important for discussion of absence of multiple crystallization/ordering events at largely different temperatures in non-isothermal FSC analysis (Figs. 2 and 3). In case of unmodified iPP, the cooling rate can be adjusted such that rather slow crystallization at temperatures higher than 330 K may be suppressed but still allows fast mesophase formation at high supercooling. In case of iPP containing a nucleating agent, however, suppression of crystallization at high temperature due to fast cooling is inevitably connected with the suppression of mesophase formation at low temperature if the characteristic times of crystallization and ordering are close-to-identical, as in the present case. As such it is not surprising that a distinct mesophase-formation peak at around 300 K, as is typically detected in neat iPP, is not observed in Fig. 2 at high cooling rate.

3.4. Reorganization of semimesomorphic β-phase nucleating agent containing iPP

The quenching experiments of Fig. 1 revealed that a variation of the rate of cooling the melt of iPP, containing β-phase nucleating agent, allows formation of different polymorphs. Cooling at a rate faster few hundred K s⁻¹ and aging at room temperature led to formation of mesophase. For unmodified iPP it is known that the mesophase transforms on slow heating at rates lower than about 30.000 K s⁻¹ to α-crystals by local chain reorganization/removal of helix reversals [51]. The mesophase in iPP containing β-phase nucleator has never been detected before, and also its stability and reorganization have not been investigated. Fig. 6 shows a series of WAXS diagrams of semimesomorphic iPP containing β-phase nucleator recorded on slow heating at a rate of 5 K min⁻¹. The front curve was recorded at 293 K and shows the characteristic halos of the mesophase of iPP. On heating, the mesophase
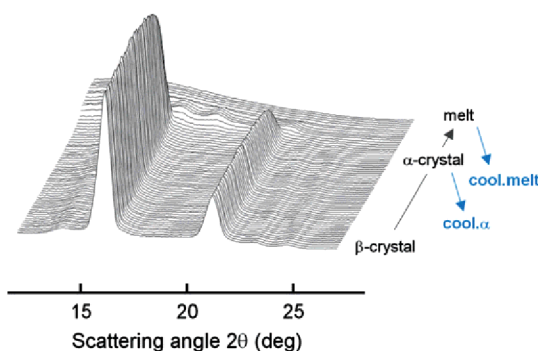
converts to α-crystals as recognized by the appearance of their characteristic diffraction peaks, with the phase transition beginning at a temperature of about 350 K. Further continuation of heating finally leads to melting of the α-crystals starting around 420 K and completed at about 430 K. As such we conclude that mesophase reorganization is not affected by the presence of β-phase nucleating agent in the iPP melt. This result is expected since it has been suggested that mesophase reorganization is a process which does not proceed via global melting and recrystallization of the melt. If this would be true then formation of β-crystals from the supercooled melt may have been observed, at least at temperatures higher than 360–370 K.

3.5. Reorganization of semicrystalline iPP containing β-crystals

Fig. 7 shows a series of WAXS curves of semicrystalline iPP containing β-crystals recorded on slow heating at a rate of 5 K min⁻¹, in order to gain knowledge about their thermal stability and/or reorganization behavior. Heating of semicrystalline iPP containing β-crystals from 293 K (front curve) to 453 K (back curve) reveals completion of melting of β-crystals at about 423 K. Continuation of heating leads to immediate formation of few α-crystals as is indicated with the evolution of their characteristic diffraction peaks of low intensity. These α-crystals melt around 435–440 K. It is worthwhile noting, that there is no indication of an overlap of the melting process of β-crystals and the formation of α-crystals. This observation is straightforward interpreted such that α-crystals are formed from the melt, and not by reorganization of β-crystals.

The low amount of α-crystals formed at a temperature of about 425 K after prior melting of β-crystals effectively nucleates α-crystal formation on cooling. If the sample is heated to a maximum temperature of 428 K, that is, to a temperature of presence of α-crystals, and then slowly cooled at a rate of 5 K min⁻¹ after a dwell time of 3 min, as is indicated with the blue arrow labeled 'cool.α' in Fig. 7, then growth of α-crystals is enforced, and the β-nucleating agent is ineffective. The formation of α-crystals on cooling along the pathway 'cool.α' in Fig. 7 has been followed by temperature-resolved WAXS and is shown in the
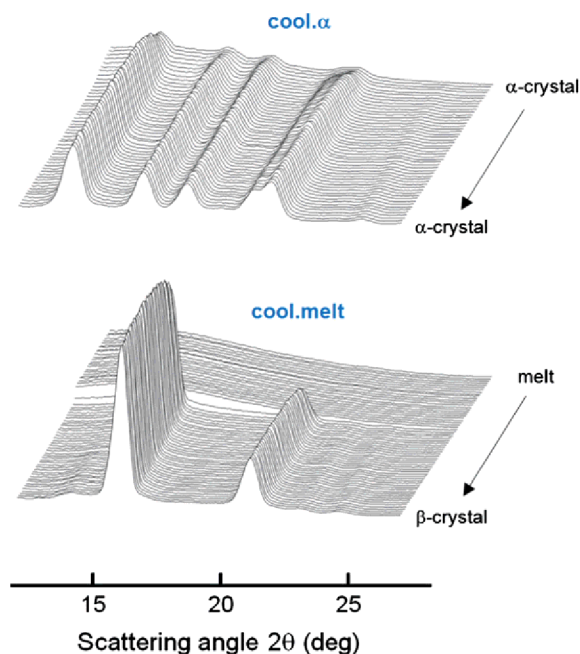
Fig. 8. Series of WAXS diagrams recorded on cooling the melt of iPP containing β-phase nucleating agent (bottom data set) or semicrystalline iPP containing β-phase nucleating agent and few α-crystals (top data set). The thermal history of these samples is shown in Fig. 7, and the cooling rate is 5 K min⁻¹.

top part of Fig. 8. The top curve has been recorded at a temperature of 428 K and reveals presence of few α-crystals. The intensity of the α-phase peaks remained constant during isothermal holding at 428 K for 3 min but increases as soon as the temperature is lowered, indicating growth of α-crystals. In contrast, if the sample is completely melted and then re-cooled at 5 K min⁻¹ after isothermal holding at 453 K for 3 min, as is indicated with the blue arrow labeled 'cool.melt' in Fig. 7, then, as expected from the experiment of Fig. 1, β-crystals are forming. The corresponding series of WAXS curves is shown in the bottom part of Fig. 8.

4. Conclusions

In the present work for the first time the polymorphism of iPP containing a β-phase nucleating agent has been investigated comprehensively as a function of the condition of melt solidification. In extension to prior work in the field of the analysis of the crystallization behavior of iPP containing purposely added heterogeneous nucleating agents we included conditions of solidification as are typical in polymer processing. It has been found that γ-quinacridone as β-phase nucleating agent is only effective on cooling the isotropic melt at rates lower than about 50–100 K s⁻¹. Faster cooling either leads to a formation of α-crystals, or complete vitrification of the supercooled liquid, depending on the cooling rate. If formation of crystals is suppressed at temperatures higher than about 320 K then annealing the supercooled melt between the glass transition temperature and 320 K leads to formation of

mesophase. It is concluded that variation of the condition of solidification the melt of iPP containing β-phase nucleating agent permits formation of β-crystals, α-crystals, and mesophase.

Isothermal crystallization experiments revealed a bimodal distribution of the rate of crystallization, as in case of unmodified iPP. The β-phase nucleating agent affects only the crystallization rate at temperatures higher than 320 K, that is, in a temperature range which in prior investigations of the crystallization behavior of iPP has been assigned to be controlled by heterogeneous nucleation. At lower temperatures, when crystallization is replaced by mesophase formation, the crystallization rate is not affected by the presence of the β-phase nucleator. This observation supports the notion that crystallization/ordering at high supercooling, at temperatures close to the glass transition temperature, is governed by homogeneous nucleation.

The polymorphism of iPP containing β-phase nucleator, that is, the formation of different ordered structures, can further be controlled by heating, or annealing at elevated temperature. Heating the mesophase leads to their reorganization to α-crystals. The mesophase–crystal phase transition which has been related to a local chain reorganization process within the ordered phase is not affected by the presence of the β-phase nucleator. The β-crystals formed on slow cooling of the melt to ambient temperature melt at temperatures below 420 K. On continuation of heating, few α-crystals form around 420–425 K which, if not melted, allow the formation of semicrystalline iPP with a large fraction of α-crystals, independent of the presence of β-phase nucleator.

Acknowledgments

References

[1] Pasquini N. Polypropylene handbook. Munich: Carl Hanser Verlag; 2005.
[2] Turner Jones A, Aizlewood JM, Beckett DR. Crystalline forms of isotactic polypropylene. Makromol Chem 1964;75:134–58.
[3] Addink EJ, Beintema J. Polymorphism of crystalline polypropylene. Polymer 1961;2:185–93.
[4] Piccarolo S. Morphological changes in isotactic polypropylene as a function of cooling rate. J Macromol Sci, Phys 1992;B31:501–11.
[5] Zia Q, Androsch R, Radusch HJ, Piccarolo S. Morphology, reorganization, and stability of mesomorphic nanocrystals in isotactic polypropylene. Polymer 2006;47:8163–72.
[6] Binsbergen FL, De Lange BGM. Morphology of polypropylene crystallized from the melt. Polymer 1968;9:23–40.
[7] Padden Jr FJ, Keith HD. Spherulitic crystallization in polypropylene. J Appl Phys. 1959;30:1479–84;
Keith HD, Padden Jr FJ, Walter NM, Wyckoff HW. Evidence for a second crystal form of polypropylene. J Appl Phys 1959;30:1485–8.
[8] Varga J. Supermolecular structure of isotactic polypropylene. J Mater Sci 1992;27:2557–79.
[9] Lotz B, Wittmann JC. The molecular origin of lamellar branching in the α (monoclinic) form of isotactic polypropylene. J Polym Sci, Polym Phys 1986;24:1541–58.

[10] Wunderlich B, Grebowicz J. Thermotropic mesophases and mesophase transitions of linear, flexible macromolecules. Adv Polym Sci 1984;60:1–59.

[11] Androsch R, Di Lorenzo ML, Schick C, Wunderlich B. Mesophases in polyethylene, polypropylene and poly(1-butene). Polymer 2010;51:4639–62.

[12] Ogawa T, Miyaji H, Asai K. Nodular structure of polypropylene. J Phys Soc Jap, Lett 1985;54:3668–70.

[13] Grubb DT, Yoon DY. Morphology of quenched and annealed isotactic polypropylene. Polym Commun 1986;27:84–8.

[14] Hsu CC, Geil PH, Miyaji H, Asai K. Structure and properties of polypropylene crystallized from the glassy state. J Polym Sci, Polym Phys 1986;24:2379–401.

[15] Zannetti R, Celotti G, Fichera A, Francesconi R. The structural effects of annealing time and temperature on the paracrystal–crystal transition in isotactic polypropylene. Makromol Chem 1969;128:137–42.

[16] O'Kane WJ, Young RJ, Ryan AJ, Bras W, Derbyshire GE, Mant GR. Simultaneous SAXS/WAXS and d.s.c. analysis of the melting and recrystallization behaviour of quenched polypropylene. Polymer 1994;35:1352–8.

[17] Wang ZG, Hsiao BS, Srinivas S, Brown GM, Tsou AH, Cheng SZD, et al. Phase transformation in quenched mesomorphic isotactic polypropylene. Polymer 2001;42:7561–6.

[18] Zia Q, Radusch HJ, Androsch R. Direct analysis of annealing of nodular crystals in isotactic polypropylene by atomic force microscopy, and its correlation with calorimetric data. Polymer 2007;48:3504–11.

[19] Zia Q, Androsch R, Radusch HJ, Ingolic E. Crystal morphology of rapidly cooled isotactic polypropylene: a comparative study by TEM and AFM. Polym Bull 2008;60:791–8.

[20] Androsch R. In situ atomic force microscopy of the mesomorphic–monoclinic phase transition in isotactic polypropylene. Macromolecules 2008;41:533–5.

[21] Varga J. Beta-modification of isotactic polypropylene: preparation, structure, processing, properties, and application. J Macromol Sci, Phys 2002;B41:1121–71.

[22] Fujiwara Y. Das Doppelschmelzverhalten der β-Phase des isotaktischen Polypropylens. Colloid Polym Sci 1975;253:273–82.

[23] Lovinger AJ, Chua JO, Gryte CG. Studies on the α and β forms of isotactic polypropylene by crystallization in a temperature gradient. J Polym Sci, Polym Phys 1977;15:641–56.

[24] Varga J, Karger-Kocsis J. Rules of supermolecular structure formation in sheared isotactic polypropylene melts. J Polym Sci, Polym Phys 1996;34:657–70.

[25] Varga J, Ehrenstein GW. Formation of β-modification in its late stage of crystallization. Polymer 1996;37:5959–63.

[26] Stocker W, Schumacher M, Graff S, Thierry A, Wittmann JC, Lotz B. Epitaxial crystallization and AFM investigation of a frustrated polymer structure: isotactic poly(propylene), β phase. Macromolecules 1998;31:807–14.

[27] Lotz B. α and β phases of isotactic polypropylene: a case of growth kinetics 'phase reentrecy' in polymer crystallization. Polymer 1998;39:4561–7.

[28] Gahleitner M, Grein C, Kheirandish S, Wolfschwenger J. Nucleation of polypropylene homo- and copolymers. Int Polym Proc 2011;26:2–20.

[29] Libster D, Aserin A, Garti N. Advanced nucleating agents for polypropylene. Polym Adv Technol 2007;18:685–95.

[30] Leugering H. Einfluß der Kristallstruktur und der Überstruktur auf einige Eigenschaften von Polypropylen. Makromol Chem 1967;109:204–16.

[31] Meille SV, Ferro DR, Brückner S, Lovinger AJ, Padden FJ. Structure of β-isotactic polypropylene: a long-standing structural puzzle. Macromolecules 1994;27:2615–22.

[32] Varga J. Melting memory effect of the β-modification of polypropylene. J Therm Anal Cal 1986;31:165–72.

[33] Luo F, Geng CZ, Wang K, Deng H, Chen F, Fu Q, et al. New understanding in tuning toughness of beta-polypropylene: the role of beta-nucleated crystalline morphology. Macromolecules 2009;42:9325–31;
Luo F, Wang K, Ning N, Geng C, Deng H, Chen F, et al. Dependence of mechanical properties on β-form content and crystalline morphology for β-nucleated isotactic polypropylene. Polym Adv Technol 2011;22:2044–54.

[34] Karger-Kocsis J, Varga J. Effects of beta-alpha transformation on the static and dynamic tensile behavior of isotactic polypropylene. J Appl Polym Sci 1996;62:291–300.

[35] Chen HB, Karger-Kocsis J, Wu JS, Varga J. Fracture toughness of alpha- and beta-phase polypropylene homopolymers and random- and block-copolymers. Polymer 2002;43:6505–14.

[36] Tjong SC, Shen JS, Li RKY. Impact fracture toughness of β-form polypropylene. Scripta Metall Mater 1995;33:503–8.

[37] Karger-Kocsis J, Varga J, Ehrenstein GW. Comparison of the fracture and failure behaviour of injection moulded alpha- and beta-polypropylene in high-speed three-point bending tests. J Appl Polym Sci 1997;64:2057–66.

[38] Jacoby P, Berstedt BH, Kissel WJ, Smith CE. Studies on the β-crystalline form of isotactic polypropylene. J Polym Sci, Polym Phys 1986;24:461–91.

[39] Grein C. Toughness of neat, rubber-modified and filled β-nucleated polypropylene: from fundamentals to applications. Adv Polym Sci 2005;188:43–104.

[40] Kardos JL, Christiansen AW, Baer E. Structure of pressure-crystallized polypropylene. J Polym Sci A-2 1966;4:777–88.

[41] Lotz B, Graff S, Wittmann JC. Crystal morphology of the γ (triclinic) phase of isotactic polypropylene and its relation to the α-phase. J Polym Sci, Polym Phys 1986;24:2017–32.

[42] Brückner S, Meille SV. Non-parallel chains in crystalline γ-isotactic polypropylene. Nature 1989;340:455–7.

[43] 12th Lähnwitzseminar on calorimetry "Interplay between nucleation, crystallization, and the glass transition", Rostock (Germany), June 10–15, 2012.

[44] Mileva D, Androsch R. Effect of co-unit type in random propylene copolymers on the kinetics of mesophase formation and crystallization. Colloid Polym Sci 2012;290:465–71.

[45] Cavallo D, Gardella L, Alfonso GC, Mileva D, Androsch R. Effect of comonomer partitioning on the kinetics of mesophase formation in random copolymers of propene and higher α-olefins. Polymer 2012;53:4429–37.

[46] De Santis F, Adamovsky S, Titomanlio G, Schick C. Isothermal nanocalorimetry of isotactic polypropylene. Macromolecules 2007;40:9026–31.

[47] Silvestre C, Cimmino S, Duraccio D, Schick C. Isothermal crystallization of isotactic poly(propylene) studied by superfast calorimetry. Macromol Rap Commun 2007;28:875–81.

[48] Fillon B, Thierry A, Wittmann JC, Lotz B. Self-nucleation and recrystallization of polymers. Isotactic polypropylene, β phase: β-α conversion and β-α growth transitions. J Polym Sci, Polym Phys 1993;31:1407–24.

[49] Grebowicz J, Lau SF, Wunderlich. The thermal properties of polypropylene. J Polym Sci, Polym Symp 1984;71:19–37.

[50] Langhe DS, Hiltner A, Baer E. Transformation of isotactic polypropylene droplets from the mesophase into the alpha-phase. J Polym Sci, Polym Phys 2011;49:1672–82.

[51] Mileva D, Androsch R, Zhuravlev E, Schick C. The temperature of melting of the mesophase of isotactic polypropylene. Macromolecules 2009;42:7275–8.

[52] Menyhárd A, Varga J, Molnár G. Comparison of different β-nucleators for isotactic polypropylene, characterisation by DSC and temperature-modulated DSC (TMDSC) measurements. J Therm Anal Calorim 2006;83:625–30.

[53] Fujiyama M. Structure and properties of injection-moldings of β-crystal nucleator-added polypropylenes. Part 3. Comparison of nucleating effect between γ-quinacridone and quinacridonequinone. Int Polym Proc 1996;11:271–4.

[54] Henning S, Adhikari R, Michler GH, Baltá-Calleja FJ, Karger-Kocsis J. Micromechanical mechanisms for toughness enhancement in β-modified polypropylene. Macromol Symp 2004;214:157–71.

[55] Gahleitner M, Bachner C, Ratajski E, Rohaczek G, Neißl W. Effects of the catalyst system on the crystallization of polypropylene. J Appl Polym Sci 1999;73:2507–15.

[56] Brucato V, La Carruba V, Piccarolo S, Titomanlio G. Polymer solidification under pressure and high cooling rates. Int Polym Proc 1999;XIV:1–8.

[57] Wunderlich B. Thermal analysis of polymeric materials. Berlin: Springer; 2005.

[58] Advanced Thermal Analysis System ATHAS. <http://www.athas.prz.rzeszow.pl>.

[59] Mathot V, Pyda M, Pijpers T, Vanden Poel G, van de Kerkhof E, van Herwaarden S, et al. The Flash DSC 1, a power compensation twin-type, chip-based fast scanning calorimeter (FSC): first findings on polymers. Thermochim Acta 2011;522:36–45.

[60] Kolesov I, Mileva D, Androsch R, Schick C. Structure formation of polyamide 6 from the glassy state by fast scanning chip calorimetry. Polymer 2011;52:5156–65.